Water Research 170 (2020) 115337

Contents lists available at ScienceDirect

Water Research

journal homepage: www.elsevier.com/locate/watres

Longitudinal dispersion of microplastics in aquatic flows using fluorometric techniques

Sarah Cook [a, *], Hui-Ling Chan [b], Soroush Abolfathi [a], Gary D. Bending [c], Hendrik Schäfer [c], Jonathan M. Pearson [a]

[a] School of Engineering, University of Warwick, Coventry, CV4 7AL, UK
[b] School of Civil and Environmental Engineering, Nanyang Technological University, Singapore
[c] School of Life Sciences, University of Warwick, Coventry, CV4 7AL, UK

ARTICLE INFO

Article history:
Received 24 May 2019
Received in revised form
25 October 2019
Accepted 23 November 2019
Available online 29 November 2019

Keywords:
Microplastics
Fluorometric tracing
Longitudinal dispersion
Uniform flow
Microplastic transport
Advection-diffusion

ABSTRACT

Microplastics are an emerging environmental contaminant. Existing knowledge on the precise transport processes involved in the movement of microplastics in natural water bodies is limited. Microplastic fate-transport models rely on numerical simulations with limited empirical data to support and validate these models. We adopted fluorometric principles to track the movement of both fluorescent dye and florescent stained microplastics (polyethylene) in purpose-built laboratory flumes with standard fibre-optic fluorometers. Neutrally buoyant microplastics behaved in the same manner as a solute (Rhodamine) and more importantly displayed classical fundamental dispersion theory in uniform open channel flow. This suggests Rhodamine, a fluorescent tracer, can be released into the natural environment with the potential to mimic microplastic movement in the water column.

1. Introduction

Microplastics (defined as plastic particles < 5 mm) are an emerging environmental contaminant and are increasingly detected in freshwater environments (Jambeck et al., 2015; Lebreton et al., 2017; Dris et al., 2018; Eriksen et al., 2018). These contaminants originate from either primary or secondary sources (Boucher and Froit, 2017). Primary sources include those intentionally manufactured for domestic and industrial purpose, a common example being abrasive microbeads in personal care products and detergents (Boucher and Froit, 2017). Secondary sources originate from the breakdown of large 'macro' plastics largely by weathering processes, including photodegradation which intensifies polymer abrasion (Gewert et al., 2015; Boucher and Froit, 2017; Rummel et al., 2017).

These emerging contaminants have gained increased interest from society, the scientific community and policymakers, yet there is little understanding as to the environmental fate and behaviour of microplastics within fluvial systems (Kooi et al., 2018). A unique feature of microplastics compared to other contaminant materials is their low density, wide size distribution and persistence within the natural environment (Kooi et al., 2018). This presents a challenge in validating models which can adequately capture their hydrodynamic behaviour in lotic ecosystems.

Eriksen et al. (2014) conservatively estimated that there are 250,000 tons of plastic floating within the world's oceans. However, a global survey by Cózar et al. (2014) estimated the global plastic load to be significantly lower and was measured to be within 7,000 to 35,000 tones. The discrepancy between Eriksen et al. (2014) and Cózar et al. (2014) has been partially attributed to the size distribution of plastic debris, with the visual methods employed by Cózar et al. (2014) unable to accurately detect sizes <1 mm in diameter (Erni-Cassola et al., 2017). An inexpensive technique to visualize microplastics using microscopy has since been developed by Erni-Cassola et al. (2017) using Nile Red (NR) fluorescence. This protocol allows the detection of small microplastics (20–1000 μm) and has proven highly effective in quantifying the main groups of microplastic polymers that are commonly found within the water column (polyethylene, PE; polypropylene, PP; polystyrene, PS; and nylon-6; Erni-Cassola et al., 2017).

* Corresponding author. School of Engineering, University of Warwick, Library Road, Coventry, CV4 7AL, UK.
E-mail address: sarah.cook@warwick.ac.uk (S. Cook).

https://doi.org/10.1016/j.watres.2019.115337

There exist many potential pathways for the transport of microplastics from source to sea (Siegfried et al., 2017). It is likely that size-selective sinks are removing micro-fragmented plastic debris during fluvial transport, which could be contributing to the uncertainty in the fate of marine microplastics (Cózar et al., 2014). The majority of microplastic studies have focused on the impact of these pollutants on marine ecosystems and their interactions with chemical pollutants (Ivar do Sul and Costa, 2014). By comparison research into the physical transport processes governing the movement of microplastics, within fluvial environments, remains far more limited. While fate transport models have attempted to explain the transport of microplastics within these systems (Law et al., 2010; Praetorius et al., 2012; Ballent et al., 2013) they remain basic and are confined to predictive models using numerical simulations (Kooi et al., 2018). Field experimental studies are also limited and are restricted to sediment (Rillig et al., 2017) and water samples collected from marine environments (Browne et al., 2010; Thompson et al., 2004; Horton et al., 2017). As such, the current knowledge pool provides a narrow understanding of the actual transport processes involved in microplastic movement in natural water bodies.

Microplastics can enter fluvial systems via numerous land-based activities including landfills, domestic waste water and industrial activities, which can be discharged into urban effluents (Dris et al., 2018; Boucher and Froit, 2017; Lebreton et al., 2017). Sewage sludge is known to contain high quantities of microplastics (Dris et al., 2018) as a large proportion is retained during water treatment (Mahon et al., 2017). A significant proportion of microplastics (i.e. PE and PP) are sourced indirectly from the weathering and fragmentation of food packaging (Dris et al., 2018). Jambeck et al., (2015) estimate that 4.4 to 12.7 million tonnes of plastic are discharged into the oceans each year as a consequence of outdated waste management strategies. The main pathways of sewage are via river systems (Boucher and Froit, 2017). Rivers transport an estimated 1.15 to 2.41 million tonnes of plastic waste to the sea (Lebreton et al., 2017). The composition of plastic polymers within rivers is mainly comprised of PE (38%), PP (24%), PVC (19%) and PS (6%) (Andrady, 2011). This data has been confirmed by several studies noting the presence of these polymers in river bed sediments across the globe (Klein et al., 2015; Zhang et al., 2015; Gasperi et al., 2014; Eerkes-Medrano et al., 2015; Hurley et al., 2018). As such, rivers represent the dominant medium connecting terrestrial microplastic sources to the marine sink. Subsequently, the processes contributing to the 'loss' of microplastics, whilst in transit, likely lies within the riverine environment.

There is a synergy in the transport mechanisms governing solutes and fine sediments in fluvial systems (i.e. sorption, diffusion and dispersion; reviews of which include: Merritt et al., 2003; Wallis, 2007; Gottschalk et al., 2009; Wallis and Guymer, 2015; Baalousha et al., 2016; Kooi et al., 2018). As such, it is not unreasonable to propose that microplastics (ones which are neutrally buoyant) could mimic solute transport in the natural environment.

The longitudinal dispersion coefficient (D_x) achieved from fluorescent dye tracing is an established technique for measuring solute pollution spread in fluvial systems (Rutherford, 1994; James, 2002; Ioannidou and Pearson, 2017). However, to date, there have been no novel methods developed to trace microplastics (Windsor et al., 2019). The NR (Nile Red) dye used by Erni-Cassola et al. (2017) to selectively stain their range of microplastics exhibits a similar fluorescence signature ($\lambda_{excitation/emission}$; 552/636 nm) to the traditional dye tracer Rhodamine, WT ($\lambda_{excitation/emission}$; 553/627 nm). As such, traditional fluorometric techniques to track Rhodamine, WT could potentially be used to track NR stained microplastics. While there have been developments in fluorescent particle tracers for surface flow measurements (Tauro et al., 2012, 2013) this has largely been achieved through the use of Particle Image Velocimetry. If the movement of microplastics is found to mimic non-toxic solute dyes (i.e. Rhodamine WT) then these hydrologic tracers have the potential to be used as a starting point in which to further study microplastic movement in a 'real-world' setting. The data generated from this could be used to support existing microplastic transport models and ultimately elucidate the fate of microplastics within a catchment. This could help to resolve the marine microplastic mass 'imbalance' and development of remediation strategies for the protection and enhancement of natural water quality. In view of this there is a necessity to evaluate the applicability of this technique for microplastic tracking specifically within river systems. The aims of this investigation were therefore threefold:

1. To evaluate the suitability of using existing NR staining methods in combination with traditional fluorometric techniques to track microplastic movement.
2. To compare the longitudinal dispersion characteristics of both Rhodamine and NR stained microplastics in laboratory scale flumes under a range of different flow regimes.
3. To elucidate the suitability of Rhodamine as a proxy for microplastic movement in uniform open channels.

2. Methodology

2.1. Microplastic staining

Polyethylene (PE) was chosen as the microplastic for this investigation. PE is neutrally buoyant (0.975 g/cm^3) and is the most ubiquitous synthetic polymer found in water bodies (Geyer et al., 2017; Lebreton et al., 2017). It is commonly used for packaging material, predominately for single use products (i.e. plastic bags, plastic films etc; Geyer et al., 2017). In addition, experimental studies have shown PE to be a vector for organic contaminants through absorption (Teuten Emma et al., 2009; Seidensticker et al., 2018) making the need to understand the movement of these microplastics of increased importance.

In the natural environment, PE is extensively fragmented into powdery fragments (Andrady, 2011) with the increased abundance of these smaller synthetic polymers of significant ecological concern (Morét-Ferguson et al., 2010). In order to replicate this material, a size diameter of PE particles in the range of 40–46 μm (powder) was used.

The microplastic staining method outlined in Erni-Cassola et al. (2017) was adapted for use in this investigation. Here, we adopt a method involving multiple incubation cycles of PE and Nile Red (NR) in order to trap the dye within the hydrophobic environment of the plastic during the process of heating (expansion) and cooling (contraction). The NR (technical grade, N3013, Sigma-Aldrich) was prepared in methanol to a working solution of 100 μg mL^{-1} by dissolving 10 mg of NR in 100 mL of methanol. 1 g of PE powder (434272, Sigma-Aldrich) was suspended in 80 ml of ultrapure water and dimethyl sulfoxide (v = 1:1) solution. The solution was incubated at room temperature (25 °C), 50 °C and 75 °C (Karakolis et al., 2019). When each temperature was reached 2 mL of NR dye was added and left to stain for 10, 20 and 30 min, respectively (Karakolis et al., 2019). After staining the particle dye solution was left overnight on an agitator at room temperature to enhance the fluorescence of the PE. Following this, the plastic content was filtered and rinsed with deionised water until the filtrate ran clear. The resulting florescent PE was then stored in 50 mL glass bottles and wrapped in aluminium foil.

2.2. Longitudinal dispersion and flow characteristics

Taylor's (1954) classical approach to describing the longitudinal dispersion of solutes in uniform flow conditions has been widely employed in numerous studies in both natural and laboratory open channel flows, with in-depth summaries of these data provided by both Fischer et al. (1979) and Rutherford (1994). It follows a Fickian diffusion-type behaviour whereby the longitudinal dispersion coefficient (D_x) in unidirectional flow conditions can be calculated from the passage of time (t) taken for the concentration of a tracer cloud (c) to move across a series of fixed points downstream from a discrete injection point. It can be presented in the form of a one-dimensional Advection-Dispersion Model (ADE). From this the method of moments can be also used to estimate a single coefficient for the longitudinal dispersion, D_x which can be derived in accordance to Fick's Law by evaluating the rate of change of variance (σ_x^2) with time, given by

$$Dx = \frac{1}{2}\left(\frac{d\sigma_x^2}{dt}\right) = \frac{1}{2}\frac{\sigma_x^2(t2) - \sigma_x^2(t1)}{t2 - t1} \tag{2.1}$$

where, $\sigma_x^2(t1)$ and $\sigma_x^2(t2)$ are the temporal variance of the tracer distributions at times t_1 *and* t_2, respectively. Fischer et al. (1979) demonstrated that equation (2.1), can be rewritten

$$Dx = \frac{u2}{2}\frac{\sigma_t^2(x2) - \sigma_x^2(x1)}{\bar{t}_2 - \bar{t}_1} \tag{2.2}$$

where

$$\frac{\sigma_t^2(xi) = \int_{t=-\infty}^{\infty}(t - \bar{t}_i)^2\,\bar{c}(x_i,t)dt}{\int_{t=-\infty}^{\infty}\bar{c}(x_i,t)dt} \tag{2.3}$$

and the centroid ($\bar{t}_i$)of the distribution is given by:

$$\bar{t}_i = \frac{\int_{t=-\infty}^{\infty} t\bar{c}(x_i,t)dt}{\int_{t=-\infty}^{\infty}\bar{c}(x_i,t)dt} \tag{2.4}$$

where $\bar{c}$ = depth averaged tracer concentration. The mean velocity is:

$$u = \frac{x_2 - x_1}{t_2 - t_1} \tag{2.5}$$

where, x is the distance along the channel (m) between the various measured positions along the channel and t is the time (seconds) for the centroid to move from one site to next.

D_x can also be theoretically derived using Elder (1959) equation which combines the shear dispersion effects of an idealised vertical velocity profile, briefly

$$D_x = 5.93hu_* \tag{2.6}$$

where, u_* is the shear velocity (m s^{-1}) and h is the mean channel depth (m), u_* can be functionally written as,

$$u_* = \sqrt{gRS_o} \tag{2.7}$$

where, g is gravity (m^2 s^{-1}), R is the hydraulic radius $\left(\frac{A}{P}\right)$, A is the area (m^2), P is the wetted perimeter (m) and S_o is the bed slope. S_o was experimentally determined for the velocities and ranged from 0.0010 to 0.0013.

Longitudinal mixing can be altered by transverse variations in flow velocity from shear effects due to channel roughness combined with turbulence and transverse mixing. These parameters are not accounted for fully in equation (2.6). Chikwendu (1986) presented a method for calculating the longitudinal dispersion in laminar or turbulent two-dimensional or pipe flow which accounts for these shear stress effects. In this method the flow is divided into N zones of parallel flow which is well mixed and moving at uniform velocity. An interzone dispersion coefficient is calculated for each zone which accounts for mixing between the zones. Longitudinal dispersion is given by.

$$D_y(N) = \sum_{j=1}^{N-1}\left(q_1 + q_2 + \ldots + q_j\right)^2\left[1 - \left(q_1 + q_2 + \ldots + q_j\right)\right]^2$$

$$\frac{x\left[v_{12\ldots J} - v_{1(j+1\ldots N]}\right]^2}{b_{j(j+1)} + \sum_{j=1}^{N} q_j e_{yj}} \tag{2.8}$$

where

$$v_{12\ldots J} = \frac{\left(\sum_{k=1}^{j} q_k\, v_k\right)}{\left(\sum_{k=1}^{j} q_k\right)} = \textit{mean velocity in the first j zones}$$

$$v_{(j+1)\ldots N} = \frac{\left(\sum_{k=j+1}^{N} q_k\, v_k\right)}{\left(\sum_{k=J+1}^{N} q_k\right)} = \textit{mean velocity in the last}(N-j)\textit{zones} \tag{2.9}$$

In this study we apply the same technique to predict the longitudinal mixing coefficient from the defined vertical distribution of the longitudinal velocity. An N zone model was created for each experimental velocity. Velocity measurements over the water column were acquired at intervals of 1.6 mm using a Nortek Vectrino (Fig. S6; Supplementary Material). An estimate of sheer stress (u_x) was determined across each velocity using the log-law relationship between the primary velocities over the depth and obtaining the gradient of the linear relationship. The intercept of this line was used to derive the roughness of the channel bed (Manning's n).

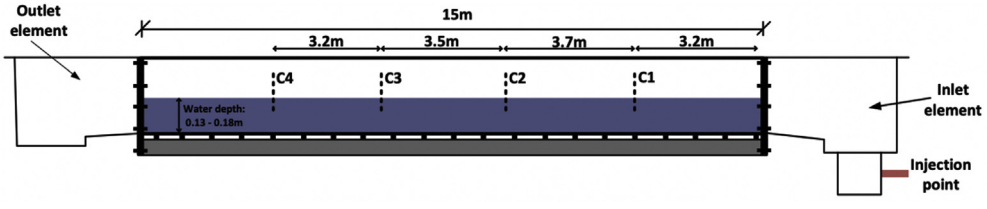

Figure 1. Plan view of the experimental flume setup (not to scale) where C1–C4 are Cyclops measurement points.

Table 1
Summary of the average longitudinal dispersion coefficient (D_x) parameters and mass difference (%). Where r^2 represents the average goodness of fit between the change in variance (σ) of the tracer against time, ± SEM is the standard error of the mean and n is the number of samples.

U(m s^{-1})	Q (m^3 s^{-1})	Dispersion coefficients dye					
		Reynolds number	$Dye_{measured}$	$D_{elder/chikwendu}$	*Mass difference (%)*	r^2	*n*
0.05	0.002	7091	0.0043 ± 0.0004	0.0042 ± 0.0005	96.33 ± 2.86	0.983	6
0.11	0.005	17703	0.0095 ± 0.0011	0.0105 ± 0.0004	92.3 ± 0.84	0.993	6
0.17	0.009	29107	0.0143 ± 0.0011	0.0173 ± 0.0003	84.33 ± 4.46	0.987	6
0.28	0.013	44527	0.0267 ± 0.0022	0.0264 ± 0.0003	93.67 ± 0.80	0.992	6
0.32	0.015	52244	0.0272 ± 0.0032	0.0304 ± 0.0002	97.33 ± 2.91	0.993	3
0.35	0.017	56424	0.0243 ± 0.0043	0.0337 ± 0.0004	82.67 ± 1.45	0.992	3
0.47	0.020	66218	0.0292 ± 0.0026	0.0367 ± 0.0021	82.21 ± 0.84	0.923	3
0.53	0.028	86842	0.0415 ± 0.0030	0.0415 ± 0.0010	86.36 ± 8.1	0.989	3
0.62	0.030	118166	0.0564 ± 0.0064	0.0448 ± 0.0025	85.05 ± 1.62	0.976	3
U(m s^{-1})	**Q (m^3 s^{-1})**	**Dispersion coefficients PE Reynolds number**	**$PE_{measured}$**	***$D_{elder/chikwendu}$***	***Mass difference (%)***	***r^2***	***n***
0.05	0.002	7091	0.0055 ± 0.0008	0.0041 ± 0.0008	94.33 ± 3.06	0.978	6
0.11	0.005	17703	0.0115 ± 0.0016	0.0106 ± 0.0007	95.33 ± 4.90	0.974	6
0.17	0.009	29107	0.0170 ± 0.0039	0.0173 ± 0.0002	90.00 ± 3.27	0.963	6
0.28	0.013	44527	0.0204 ± 0.0014	0.0268 ± 0.0001	83.17 ± 3.14	0.985	6
0.32	0.015	52244	0.0256 ± 0.0026	0.0304 ± 0.0003	98.67 ± 7.84	0.996	3
0.35	0.017	56424	0.0329 ± 0.0015	0.0335 ± 0.0003	86.00 ± 3.46	0.999	3
0.47	0.020	66218	0.0262 ± 0.0027	0.0367 ± 0.0021	86.00 ± 1.96	0.944	3
0.53	0.028	86842	0.0447 ± 0.0044	0.0415 ± 0.0010	82.13 ± 5.1	0.934	3
0.62	0.030	118166	0.0506 ± 0.0094	0.0448 ± 0.0025	89.70 ± 5.9	0.923	3

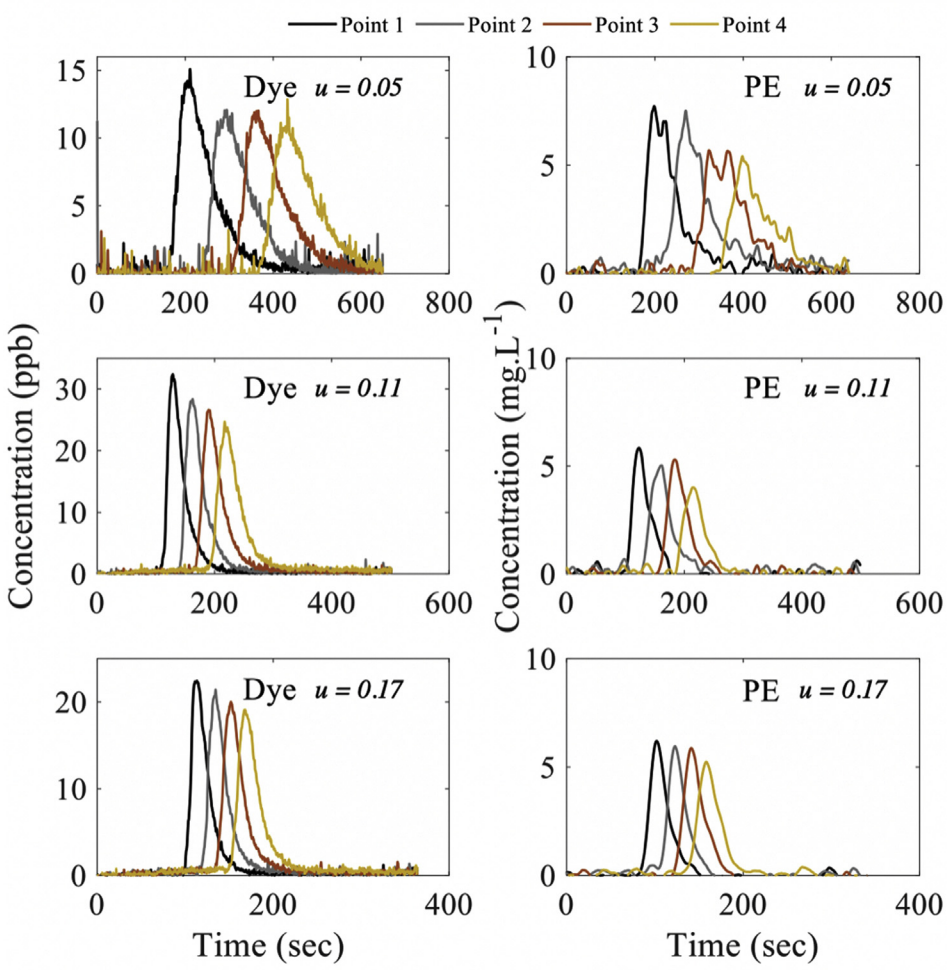

Fig. 2. Response curves of the instantaneous tracer injections for dye and microplastic particles (PE) plotted as concentration against time elapsed for vehicles (u) 0.005,0.11,0.17 ms^{-1}

These parameters, alongside an assumed Von Karman constant of 0.41 were used to define the specific channel conditions. By applying Chikwendu's (1986) methodology and adopting the measured longitudinal velocity, with suitable vertical exchange coefficients, the overall calculated dispersion in the longitudinal direction can be determined.

2.3. Experiment flume conditions

All tracer experiments were conducted in a 15-m long, 300-mm wide recirculating tilting Armfield flume (Fig. 1). Full details of the experimental set-ups are presented in Table 1 alongside some of the results. Uniform flow was established at average velocities of 0.05–0.62 m s^{-1} by adjusting the flume slope and tailgate. This range was chosen to approximate velocities experienced by UK rivers (Guymer, 2002). Reynolds numbers (R_e) were calculated for each velocity to determine the boundary conditions for each experimental injection and ranged from 7091 to over 118,000 (Table 1), indicative of turbulent flow conditions, given by

$$R_e = \frac{uh}{v} \tag{2.10}$$

where u is the velocity (m s^{-1}), h is the mean channel depth (m) and v the kinematic viscosity (m^2 s^{-1}).

Water depth was noted before each injection and varied between 135-mm to 180-mm, within the flume, and was confirmed using point gauges along the length of the flume. Dye and fluorescent PE tracing were carried out using four submerged Turner Design Cyclops-7 fluorometers positioned at fixed points (1.97-m, 5.63-m, 9.13-m, 12.3-m) downstream from the injection point (Fig. 1). The instruments were fixed at a position approximately 50 mm from the water surface and at a 20° angel to ensure maximum detection of the tracer cloud in the centre of flow and encompass its distribution at depth. The Cyclops's were connected to an automatic recorder which logged changes in the voltage of the water column (as a consequence of fluorescence) over a 0.5 s time interval.

Manual pulse injections of both dye and fluorescent PE were made directly into the inlet pipe of the flume to ensure the that the contaminant was well mixed within the flow. For each instantaneous injection of fluorescent PE approximately 1 g was injected combined with a small amount of water (<10 ml). It was then injected into the inlet pipe of the flume where it travelled approximately 1 m, mixing with the turbulent inflow water, before entering the flume (Fig. 1). This was performed to ensure complete mixing before entry into the flume. Between tracer injections the injector point was flushed three times with water to ensure no cross contamination of Rhodamine and PE. For each dye injection 3 ml of Rhodamine with a concentration of 10^6 ppb was used. Three to six discrete injections were undertaken for each discharge for

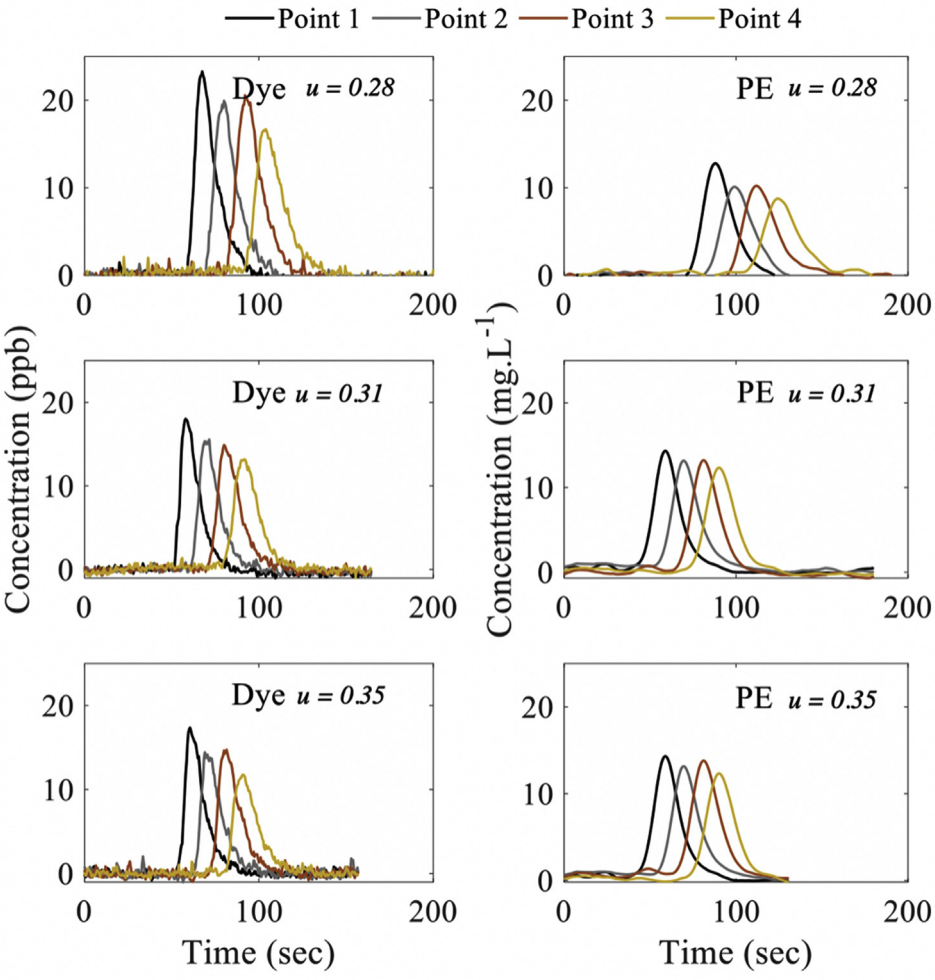

Fig. 3. Response curves of the instantaneous tracer injections for dye and microplastic (PE) plotted as concentration against time elapsed for discharges (u) 0.28, 0.31, 0.35 ms^{-1}

both tracers. The voltages recorded for both Rhodamine and fluorescent PE were then converted into concentrations (ppb and mg L^{-1}, respectively) using linear calibration curves ($r^2 > 0.99$).

The cyclops instruments have a detection level of up to 15 cm from the optical sensor. Hence, it was assumed that the majority of the water column (set at 135-mm to 180-mm) would be detected. However, to check that the PE particles and dye adhered to the assumptions of the one-dimensional ADE (i.e. that they reached a homogenous lateral and vertical distribution in the water column; particularly PE which has a naturally low density) the cyclops instruments were positioned lying down, at the same positions, approximately 20-mm from the flume base. Three manual pulse injections of both the dye and PE were made, as discussed previously, across the range of average velocities tested i.e. 0.05, 0.17, 0.35 and 0.62 m s^{-1}. For each test the dispersion coefficients were determined and compared to the corresponding data generated from the cyclops instruments positioned at the top of the water column (Supplementary Material; Fig. S1). The concentrations were also compared (Supplementary Material; Fig. S2 – S5). Overall, these tests revealed similar corresponding dispersion coefficients generated at both the top and bottom measured positions with no significant differences reported. Concentrations were also comparable suggesting sufficient mixing of both the dye and PE across velocities.

2.4. Data processing

Before analysis the raw concentration data was processed by removing the background concentration. This was defined as the mean concentration during the first 30 s before the tracer was injection. The microplastic injections generated a more scattered dispersion band (Figs. S7a–S12a, Supplementary Material), especially for lower discharges (2–5 Ls^{-1}). This could be attributed to the PE particles generating discrete pockets of fluorescence compared to the well dissolved Rhodamine dye. To address this a smooth curve was drawn through the points, compensating for background fluorescence and occasional anomalies (Figs. S7b - S12b, Supplementary Material).

The standard ADE coefficients were generated from the temporal concentration distribution of each tracer injection. The cut-off value of the distribution curve was defined as the point where the concentration at the tail of the curve reached approximately 5% of the peak concentration. Before analysis the background concentration was removed by interpolating a line between the leading and end tails of the concentration distribution curves. The decision on where to interpolate this line from (i.e. cut-off points) was i) similar travel times (standard deviation < 3%, dye <5%, PE) between the centroids of the distribution for the repeat injections and ii) r^2 value of >0.95 for the linear variance-time plot.

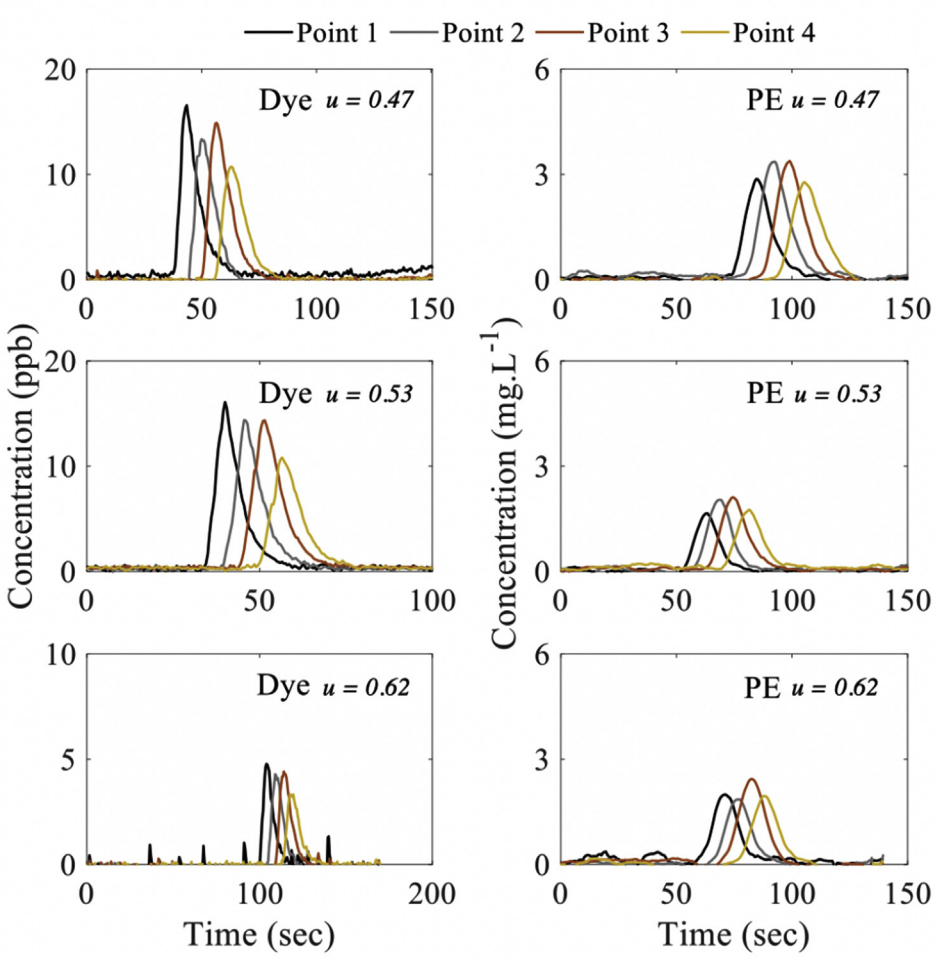

Fig. 4. Response curves of the instantaneous tracer injections for dye and microplastic (PE) plotted as concentration against time elapsed for discharges (u) 0.47, 0.53, 0.62 ms^{-1}

The travel time (t, *seconds*) of the passage of the centroid (μ) of the tracer cloud between measurement sites was calculated to understand how it changed from the upstream ($_i$) profile to downstream ($_{ii}$), briefly

$$t = \mu_{ii} - \mu_i \tag{2.11}$$

2.5. Data analysis

The data was processed using MATLAB and statistical analysis performed in GraphPad Prism v7. Normality was tested using the Shapiro-Wilk test. The threshold level for significance was set at a probability of 0.05. The relationship between variables was tested using linear regression and root mean square error (RMSE).

3. Results

The velocities calculated ranged from 0.05 to 0.65 m s^{-1} and were grouped into the following categories based on their averages: 0.05, 0.11, 0.17, 0.28, 0.32, 0.35, 0.47, 0.53, 0.62 m s^{-1}. The response curves of the instantaneous tracer injections were plotted as concentration against time elapsed (Figs. 2–4). All profiles exhibit a Gaussian shape distribution and were conservative under uniform flow conditions. The travel times of the temporal concentration profiles were plotted in relation to velocity (Supplementary Fig. S13) and revealed that the dye and PE tracers move downstream at similar rates across all velocity. Centroid travel times were plotted in relation to velocity (Fig. S13; Supplementary Material) and show an expected inverse response .

The longitudinal dispersion coefficients obtained using the standard method of moments were plotted against the corresponding velocity (Fig. 5). The coefficients range from 0.0034 to 0.0511 m^2 s^{-1} for the dye and 0.0030–0.0690 m^2 s^{-1} for the PE particles. Both the dye and PE longitudinal dispersion coefficients increase linearly with velocity with r^2 values of 0.85 and 0.75, respectively (Fig. 5b). When the mean dispersion coefficients were plotted against velocity a higher linearity is recorded of 0.93 and 0.90 for the dye and PE, respectively (Fig. 5a). In general, the PE particles dispersed at a faster rate than the dye except at lower velocities (<0.28 m s^{-1}) (Table 1). However, further comparison of the raw dispersion coefficient data revealed that there was no statistically significant difference between dispersion behaviour of the tracer and particle mediums (Welch's t-test $p > 0.05$).

The longitudinal dispersion coefficients generated from the trace experiments was compared with the theoretical D_X values obtained using both Elder (1959) empirical ADE model and the Chikwendu (1986) model (Fig. 6). As expected, the analytical methodology of Elder and the numerical methodology of Chikwendu gave similar results. Overall, there is a good fit between the measured experimental values and the theoretical dispersion coefficient constants. This was confirmed by a one-way ANOVA with no significant difference identified between the experimental and theoretical dispersion data across all velocities ($p > 0.05$). Exceptions to this trend were at velocities of 0.44–0.49 m s^{-1} when the theoretical values were, in general, significantly greater than the measured dye and PE dispersion coefficients (Fig. 6). Two anomalous dispersion coefficients were also observed for the dye, at a velocity of 0.58 m s^{-1}, and PE, for a velocity of 0.65 m s^{-1}, which were significantly greater than their respective theoretical values.

The strong agreement between the best fit line for both PE and dye and theoretical predictions is further reinforced by a comparison of the root mean square error (RMSE) data (Table 2). Here, it is clear that the dye had a stronger agreement with the theoretical values, except for a velocity of 0.35 and 0.62 m s^{-1}. In general, the dye and PE dispersion coefficients display a closer agreement to one another at lower velocities (Table 2). However, overall all RMSEs were very strong across and between the experimental and theoretical coefficients.

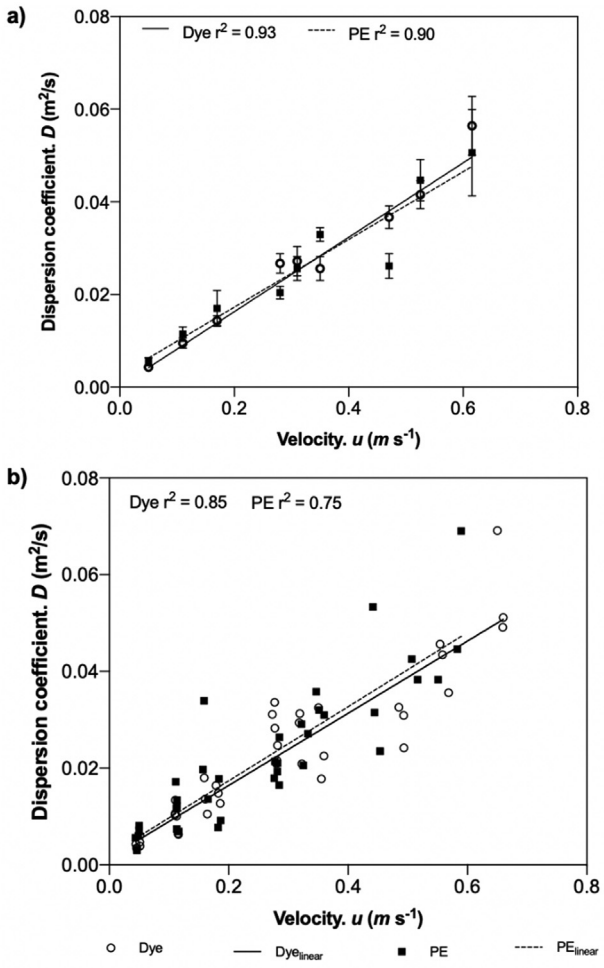

Fig. 5. Dispersion coefficients for the dye and microplastic (PE) plotted in relation to (a) mean dispersion coefficient (±standard error of the mean) versus categorized discharges values and (b) individually calculated dispersion coefficients versus measured velocity.

4. Discussion

The stained microplastics exhibited a stable fluorescence allowing detection and tracking in the water column. Previous research has suggested that microplastic particles are likely to behave in a similar manner to other particulate matter (i.e. soil particles and organic matter) with similar physical characteristics (i.e. density, size and shape; Nizzetto et al., 2016; Kooi et al., 2018). The data suggest that PE microplastics (40–46 μm powder form) disperse in a similar manner to Rhodamine dye and comply with the assumption of fundamental dispersion theory in a straight channel under uniform flow conditions. This is further supported by the comparative statistics. This is likely attributable to the straight laboratory flume satisfying Elder and Chikwendu's assumption of an idealised velocity profile.

It is encouraging that both the PE and dye data plot on a similar linear trajectory across all experimental velocities when tested in uniform open flow conditions. These velocities are representative

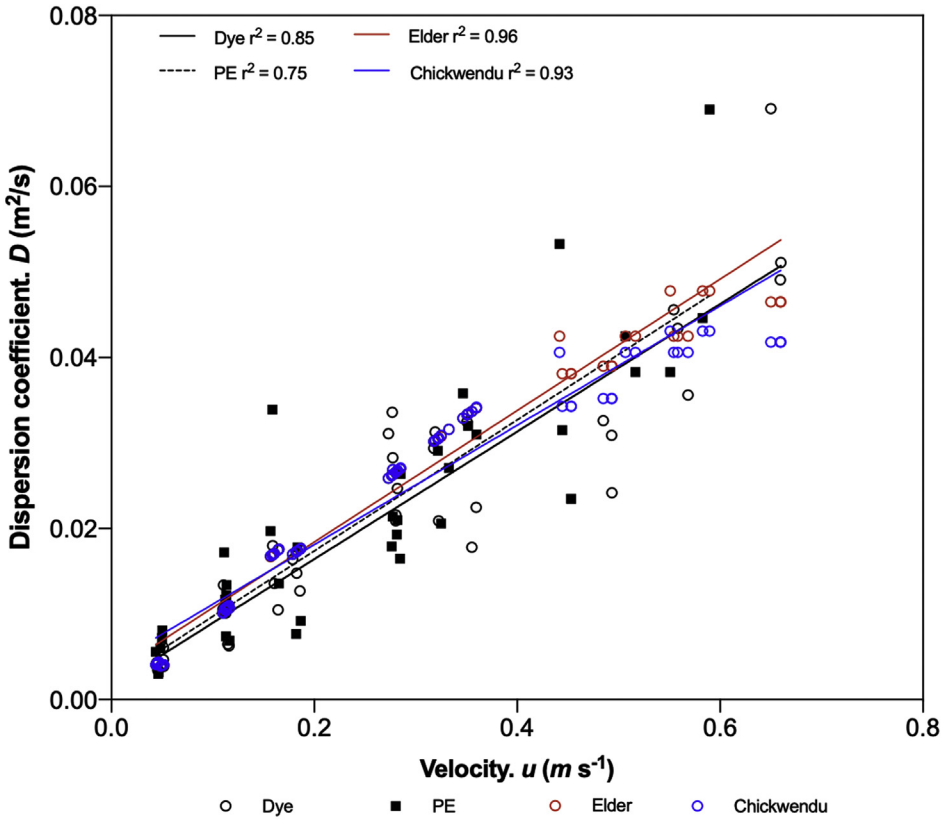

Fig. 6. Individually calculated dispersion coefficients for the dye, microplastic (PE) and theoretical values from Elder/Chikwendu plotted in relation to the measured velocity.

Table 2
Comparison of dispersion coefficients, using the root mean square error (RMSE), between the dye, microplastic and theoretical approaches across the different discharges.

U (m s^{-1})	Q (m^3 s^{-1})	Dye vs Elder/Chikwendu	PE vs Elder/Chikwendu	PE vs dye
0.05	0.002	0.0004	0.0010	0.0009
0.11	0.005	0.0012	0.0015	0.0023
0.17	0.009	0.0016	0.0036	0.0036
0.28	0.013	0.0023	0.0029	0.0031
0.32	0.015	0.0033	0.0038	0.0043
0.35	0.017	0.0066	0.0015	0.0062
0.47	0.019	0.0105	0.0126	0.0043
0.53	0.025	0.0044	0.0067	0.0066
0.62	0.028	0.0134	0.0125	0.0197

of UK rivers. However, the physical and structural diversity of microplastics in the environment is abundant (Windsor et al., 2019) and so their movement is compounded by the non-uniformities of natural river reaches, both within and across ecosystems (i.e. meanders, dead zones and vegetation). This is emphasised by Rutherford (1994) who reports longitudinal dispersion coefficients of between $30hu_*$ to $3000hu_*$ in natural river channels,. This is significantly greater than Elder's (1959) theoretical value estimated for the boundary conditions of the flow channel used in the experiments. Obtaining more data for PE particles and dye across more representative complex river environments (i.e. with a river bed) may provide some guidance and insight into how this specific microplastic behaves in a natural river system. Nevertheless, the methodology presented within this paper provides a foundational starting point to track and theoretically describe the movement of microplastics using existing solute transport technology.

We acknowledge the limitations of our data. Firstly, only one specific type and size of microplastic was tested. The inclusion of a wider range of plastics with different densities and sizes are required to elucidate the processes and validate the wider applicability of this methodology. For example, flakier microplastic particles generated primarily from car tyre abrasion (Lechner et al., 2014) are likely to disperse differently due to increased drag. Secondly, the microplastics tested were 'pure' polymers with no biofilm growth. In reality most microplastics are colonized by microbes, a phenomenon which has been observed in marine (Long et al., 2015; Fazey and Ryan, 2016; Michels et al., 2018) and more recently freshwater environments (Parrish and Fahrenfeld, 2019). Biofouling can change the hydrodynamics and size of microplastics which can cause even buoyant polymers to sink and settle in sediment due to aggregation (Besseling et al., 2017).

The environmental fate of microplastics is an emerging field of science. As such, there is only one conceptual fate-transport model, to our knowledge, that describes microplastic transport in rivers (Nizzetto et al., 2016). Model progression is largely limited by a lack of empirical data. However, this, in turn, is constrained by the

legalities and environmental implications of releasing microplastics into the natural environment. This investigation provides a first attempt to trace the movement of neutrally buoyant microplastics in the water column, using existing solute transport technology and theory. Furthermore, this method uses a microplastic polymer (PE) which is ubiquitous within river environments and considered to be an environmental concern (Morét-Ferguson et al., 2010; Erni-Cassola et al., 2017; Kooi et al., 2018). We show that a harmless fluorescent tracer (in admissible doses; Smart and Laidlaw, 1977; Rowinski and Chrzanowski, 2011), which can be safely released into the natural environment, has the potential to be used a proxy for the movement of neutrally buoyant microplastics in uniform open channel flow. This methodology could help to bridge current knowledge gaps including: the residence times in fluvial systems, transport pathways and sinks (Clark et al., 2016; Galloway et al., 2017; Windsor et al., 2019) and thus, validate existing transport models.

5. Conclusions

The movement of neutrally buoyant microplastics (polyethylene) can be tracked in laboratory flume conditions using fluorometric techniques combined with existing solute transport technology. Neutrally buoyant microplastic particles behaved in a similar manner to solutes and followed theoretical dispersion theory in uniform open channel flow. As such, previously developed fluorescent tracking techniques using a harmless tracer, which can be safely released into the natural environment (in admissible doses), has the potential to be used as a starting point in which to further study microplastic movement in the natural environment. Additional data related to this publication is available from the University of Warwick data archive at http://wrap.warwick.ac.uk

Declaration of competing interest

The authors declare that they have no known competing financial interests or personal relationships that could have appeared to influence the work reported in this paper.

Acknowledgments

Funding was provided by the Natural Environmental Research Council (grant NE/R003645/1) and University of Warwick Global Challenges Research Catalyst Fund. We gratefully acknowledge I.Baylis, our Civil Engineering technician, for help with the experimental set up and design and helpful discussions with colleagues including J.A. Christie-Oleza (University of Warwick Life Sciences).

Appendix A. Supplementary data

Supplementary data to this article can be found online at https://doi.org/10.1016/j.watres.2019.115337.

References

Andrady, A.L., 2011. Microplastics in the marine environment. Mar. Pollut. Bull. 62 (8), 1596–1605.
Baalousha, M., Cornelis, G., Kuhlbusch, T.A.J., Lynch, I., Nickel, C., Peijnenburg, W., van den Brink, N.W., 2016. Modeling nanomaterial fate and uptake in the environment: current knowledge and future trends. Environ. Sci.: Nano 3 (2), 323–345.
Ballent, A., Pando, S., Purser, A., Juliano, M.F., Thomsen, L., 2013. Modelled transport of benthic marine microplastic pollution in the Nazaré Canyon. Biogeosciences 10 (12), 7957–7970.
Besseling, E., Quik, J.T.K., Sun, M., Koelmans, A.A., 2017. Fate of nano- and microplastic in freshwater systems: a modeling study. Environ. Pollut. 220, 540–548.
Boucher, J., Froit, D., 2017. Primary Microplastics in the Oceans: A Global Evaluation of Sources. IUCN, Gland, Switzerland.
Browne, M.A., Galloway, T.S., Thompson, R.C., 2010. Spatial patterns of plastic debris along estuarine shorelines. Environ. Sci. Technol. 44 (9), 3404–3409.
Chikwendu, S.C., 1986. Application of a slow-zone model to contaminant dispersion in laminar shear flows. Int. J. Eng. Sci. 24 (6), 1031–1044.
Clark, J.R., Cole, M., Lindeque, P.K., Fileman, E., Blackford, J., Lewis, C., Lenton, T.M., Galloway, T.S., 2016. Marine microplastic debris: a targeted plan for understanding and quantifying interactions with marine life. Front. Ecol. Environ. 14 (6), 317–324.
Cózar, A., Echevarría, F., González-Gordillo, J.I., Irigoien, X., Úbeda, B., Hernández-León, S., Palma, Á.T., Navarro, S., García-de-Lomas, J., Ruiz, A., Fernández-de-Puelles, M.L., Duarte, C.M., 2014. Plastic debris in the open ocean, 111 (28), 10239–10244.
Dris, R., Gasperi, J., Tassin, B., 2018. In: Wagner, M., Lambert, S. (Eds.), Freshwater Microplastics : Emerging Environmental Contaminants?. Springer International Publishing, Cham.
Eerkes-Medrano, D., Thompson, R.C., Aldridge, D.C., 2015. Microplastics in freshwater systems: a review of the emerging threats, identification of knowledge gaps and prioritisation of research needs. Water Res. 75, 63–82.
Elder, J.W., 1959. The dispersion of marked fluid in turbulent shear flow. J. Fluid Mech. 5 (4), 544–560.
Eriksen, M., Thiel, M., Prindiville, M., Kiessling, T., 2018. In: Wagner, M., Lambert, S. (Eds.), Freshwater Microplastics : Emerging Environmental Contaminants?. Springer International Publishing, Cham.
Eriksen, M., Lebreton, L.C.M., Carson, H.S., Thiel, M., Moore, C.J., Borerro, J.C., Galgani, F., Ryan, P.G., Reisser, J., 2014. Plastic pollution in the world's oceans: more than 5 trillion plastic pieces weighing over 250,000 tons afloat at sea. PLoS One 9 (12), e111913.
Erni-Cassola, G., Gibson, M.I., Thompson, R.C., Christie-Oleza, J.A., 2017. Lost, but found with nile red: a novel method for detecting and quantifying small microplastics (1 mm to 20 μm) in environmental samples. Environ. Sci. Technol. 51 (23), 13641–13648.
Fazey, F.M.C., Ryan, P.G., 2016. Biofouling on buoyant marine plastics: an experimental study into the effect of size on surface longevity. Environ. Pollut. 210, 354–360.
Fischer, H.B., List, E.J., Koh, R.C.Y., Imberger, J., Brooks, N.H., 1979. In: Fischer, H.B., List, E.J., Koh, R.C.Y., Imberger, J., Brooks, N.H. (Eds.), Mixing in Inland and Coastal Waters. Academic Press, San Diego, pp. 104–147.
Galloway, T.S., Cole, M., Lewis, C., 2017. Interactions of microplastic debris throughout the marine ecosystem. Nat. Ecol. Evol. 1, 0116.
Gasperi, J., Dris, R., Bonin, T., Rocher, V., Tassin, B., 2014. Assessment of floating plastic debris in surface water along the Seine River. Environ. Pollut. 195, 163–166.
Gewert, B., Plassmann, M.M., MacLeod, M., 2015. Pathways for degradation of plastic polymers floating in the marine environment. Environ. Sci. Process. Impacts 17 (9), 1513–1521.
Geyer, R., Jambeck, J.R., Law, K.L., 2017. Production, use, and fate of all plastics ever made. Sci. Adv. 3 (7), e1700782.
Gottschalk, F., Sonderer, T., Scholz, R.W., Nowack, B., 2009. Modeled environmental concentrations of engineered nanomaterials (TiO_2, ZnO, Ag, CNT, fullerenes) for different regions. Environ. Sci. Technol. 43 (24), 9216–9222.
Guymer, I., 2002. A National Database of Travel Time, Dispersion and Methodologies for the Protection of River Abstractions. The Environment Agency, Bristol.
Horton, A.A., Walton, A., Spurgeon, D.J., Lahive, E., Svendsen, C., 2017. Microplastics in freshwater and terrestrial environments: evaluating the current understanding to identify the knowledge gaps and future research priorities. Sci. Total Environ. 586, 127–141.
Hurley, R., Woodward, J., Rothwell, J.J., 2018. Microplastic contamination of river beds significantly reduced by catchment-wide flooding. Nat. Geosci. 11 (4), 251–257.
Ioannidou, V.G., Pearson, J.M., 2017. Case studies investigating hydraulic parameters in full-scale constructed wetlands. Eur. Water 58, 151–158.
Ivar do Sul, J.A., Costa, M.F., 2014. The present and future of microplastic pollution in the marine environment. Environ. Pollut. 185, 352–364.
Jambeck, J.R., Geyer, R., Wilcox, C., Siegler, T.R., Perryman, M., Andrady, A., Narayan, R., Law, K.L., 2015a. Marine pollution. Plastic waste inputs from land into the ocean. Science 347, 766–771.
James, I.D., 2002. Modelling pollution dispersion, the ecosystem and water quality in coastal waters: a review. Environ. Model. Softw 17 (4), 363–385.
Karakolis, E.G., Nguyen, B., You, J.B., Rochman, C.M., Sinton, D., 2019. Fluorescent dyes for visualizing microplastic particles and fibers in laboratory-based studies. Environ. Sci. Technol. Lett. 6 (6), 334–340.
Klein, S., Worch, E., Knepper, T.P., 2015. Occurrence and spatial distribution of microplastics in river shore sediments of the rhine-main area in Germany. Environ. Sci. Technol. 49 (10), 6070–6076.
Kooi, M., Besseling, E., Kroeze, C., Van Wezel, A.P., Koelmans, A.A., 2018. In: Wagner, M., Lambert, S. (Eds.), Freshwater Microplastics : Emerging Environmental Contaminants?. Springer International Publishing, Cham.
Law, K.L., Morét-Ferguson, S., Maximenko, N.A., Proskurowski, G., Peacock, E.E., Hafner, J., Reddy, C.M., 2010. Plastic accumulation in the north atlantic subtropical gyre. Science 329 (5996), 1185–1188.
Lebreton, L.C.M., van der Zwet, J., Damsteeg, J.W., Slat, B., Andrady, A., Reisser, J., 2017. River plastic emissions to the world's oceans. Nat. Commun. 8, 15611.
Lechner, A., Keckeis, H., Lumesberger-Loisl, F., Zens, B., Krusch, R., Tritthart, M.,

Glas, M., Schludermann, E., 2014. The Danube so colourful: a potpourri of plastic litter outnumbers fish larvae in Europe's second largest river. Environ. Pollut. 188, 177–181.
Long, M., Moriceau, B., Gallinari, M., Lambert, C., Huvet, A., Raffray, J., Soudant, P., 2015. Interactions between microplastics and phytoplankton aggregates: impact on their respective fates. Mar. Chem. 175, 39–46.
Mahon, A.M., O'Connell, B., Healy, M.G., O'Connor, I., Officer, R., Nash, R., Morrison, L., 2017. Microplastics in sewage sludge: effects of treatment. Environ. Sci. Technol. 51 (2), 810–818.
Merritt, W.S., Letcher, R.A., Jakeman, A.J., 2003. A review of erosion and sediment transport models. Environ. Model. Softw 18 (8), 761–799.
Michels, J., Stippkugel, A., Lenz, M., Wirtz, K., Engel, A., 2018. Rapid aggregation of biofilm-covered microplastics with marine biogenic particles. Proc. R. Soc. Biol. Sci. 285 (1885), 20181203.
Morét-Ferguson, S., Law, K.L., Proskurowski, G., Murphy, E.K., Peacock, E.E., Reddy, C.M., 2010. The size, mass, and composition of plastic debris in the western North Atlantic Ocean. Mar. Pollut. Bull. 60 (10), 1873–1878.
Nizzetto, L., Bussi, G., Futter, M.N., Butterfield, D., Whitehead, P.G., 2016. A theoretical assessment of microplastic transport in river catchments and their retention by soils and river sediments. Environ. Sci.: Process. Impacts 18 (8), 1050–1059.
Parrish, K., Fahrenfeld, N.L., 2019. Microplastic biofilm in fresh- and wastewater as a function of microparticle type and size class. Environ. Sci.: Water Res. Technol. 5 (3), 495–505.
Praetorius, A., Scheringer, M., Hungerbühler, K., 2012. Development of environmental fate models for engineered nanoparticles—a case study of TiO_2 nanoparticles in the rhine river. Environ. Sci. Technol. 46 (12), 6705–6713.
Rillig, M.C., Ingraffia, R., de Souza Machado, A.A., 2017. Microplastic Incorporation into Soil in Agroecosystems, vol. 8, 1805.
Rowiński, P.M., Chrzanowski, M.M., 2011. Influence of selected fluorescent dyes on small aquatic organisms. Acta Geophys. 59 (1), 91–109.
Rummel, C.D., Jahnke, A., Gorokhova, E., Kühnel, D., Schmitt-Jansen, M., 2017. Impacts of biofilm formation on the fate and potential effects of microplastic in the aquatic environment. Environ. Sci. Technol. Lett. 4 (7), 258–267.
Rutherford, J.C., 1994. River Mixing. Wiley, New York.
Seidensticker, S., Grathwohl, P., Lamprecht, J., Zarfl, C., 2018. A combined experimental and modeling study to evaluate pH-dependent sorption of polar and non-polar compounds to polyethylene and polystyrene microplastics. Environ. Sci. Eur. 30 (1), 30.
Siegfried, M., Koelmans, A.A., Besseling, E., Kroeze, C., 2017. Export of microplastics from land to sea. A modelling approach. Water Res. 127, 249–257.
Smart, P.L., Laidlaw, I.M.S., 1977. An evaluation of some fluorescent dyes for water tracing. Water Resour. Res. 13 (1), 15–33.
Tauro, F., Grimaldi, S., Petroselli, A., Porfiri, M., 2012. Fluorescent particle tracers for surface flow measurements: a proof of concept in a natural stream. Water Resour. Res. 48 (6).
Tauro, F., Porfiri, M., Grimaldi, S., 2013. Fluorescent eco-particles for surface flow physics analysis. AIP Adv. 3 (3), 032108.
Taylor Geoffrey, I., 1954. The dispersion of matter in turbulent flow through a pipe. Proc. R. Soc. Lond. Ser A Math. Phys. Sci. 223 (1155), 446–468.
Teuten Emma, L., Saquing Jovita, M., Knappe Detlef, R.U., Barlaz Morton, A., Jonsson, S., Björn, A., Rowland Steven, J., Thompson Richard, C., Galloway Tamara, S., Yamashita, R., Ochi, D., Watanuki, Y., Moore, C., Viet Pham, H., Tana Touch, S., Prudente, M., Boonyatumanond, R., Zakaria Mohamad, P., Akkhavong, K., Ogata, Y., Hirai, H., Iwasa, S., Mizukawa, K., Hagino, Y., Imamura, A., Saha, M., Takada, H., 2009. Transport and release of chemicals from plastics to the environment and to wildlife. Philos. Trans. R. Soc. Biol. Sci. 364 (1526), 2027–2045.
Thompson, R.C., Olsen, Y., Mitchell, R.P., Davis, A., Rowland, S.J., John, A.W.G., McGonigle, D., Russell, A.E., 2004. Lost at sea: where is all the plastic? Science 304 (5672), 838-838.
Wallis, S.G., Guymer, I., 2015. Applications of the concept of river tracer data similarity. Water Environ. J. 29 (2), 190–201.
Wallis, S.J.A.G., 2007. The numerical solution of the Advection-Dispersion Equation: a review of some basic principles. Acta Geophys. 55 (1), 85–94.
Windsor, F.M., Durance, I., Horton, A.A., Thompson, R.C., Tyler, C.R., Ormerod, S.J., 2019. A catchment-scale perspective of plastic pollution. Glob. Chang. Biol. 25 (4), 1207–1221.
Zhang, K., Gong, W., Lv, J., Xiong, X., Wu, C., 2015. Accumulation of floating microplastics behind the three Gorges Dam. Environ. Pollut. 204, 117–123.